Characterization and Application of Self-Assembly Porphyrin with Four "Clips" on Gold Surface

Jiandong Yang,[†,‡] Minrui Li,[†,‡] Hongxiang Li,[‡] Yanlian Yang,[§] Yoshiaki Kashimura,[⊥] Chen Wang,[§] Keiichi Torimitsu,[⊥] Xiaoquan Lu,*[,†] and Wenping Hu*[,‡]

College of Chemistry and Chemical Engineering, Northwest Normal University, Lanzhou 730070, People's Republic of China, Laboratory of Organic Solids, Institute of Chemistry, Chinese Academy of Sciences, Beijing 100080, People's Republic of China, National Center for Nanoscience and Technology, Beijing 100190, People's Republic of China, and NTT Basic Research Laboratories, NTT Corporation, 3-1 Morinosato Wakamiya, Atsugi, Kanagawa 243-0198, Japan

Received: March 7, 2010; Revised Manuscript Received: May 31, 2010

Self-assembled monolayers (SAMs) of thiol-derivatized porphyrin molecules on Au substrate have attracted extensive interest for use in sensing, molecular recognition, and molecular electronics. Here, we synthesized tetra[*p*-(3-mercaptopropyloxy)phenyl]porphyrin (PPS_4) with four "clips" for SAMs. The results demonstrated that PPS_4 could form excellent SAMs on gold surface wherein the molecules oriented on substrates with a tilted angle. Self-assembled nanojunctions of PPS_4 were fabricated by using gold nanogap electrodes (gap width: ca. 100 nm), which exhibited nonlinear current−voltage characteristics, indicating tunneling injection of current from Au electrodes into PPS_4. With the light on/off, the nanojunctions switched between low/high impedance states as nanometer scaled photoswitchers.

Introduction

Self-assembled porphyrins widely exist in photosynthetic proteins serving as active species in the initial steps of light-energy conversion.[1−3] It is also well-known that thiols and disulfides could be covalently linked to the surface of gold by Au−S binding to form highly ordered self-assembled monolayers (SAMs).[4−7] SAMs of thiol-derivatized porphyrins on Au substrate have attracted extensive interest because of the unique optical/electronic properties of the SAMs as well as their excellent stability,[8−12] so that they have been broadly applied in sensing,[13−15] molecular recognition,[16−20] electrocatalytic reduction,[21−24] and molecular electronics.[25−27] To our knowledge, most available studies have been on SAMs of porphyrins wherein each molecule has only one thiol/thioacetate-end-functionalized group (i.e., single "clip"), and few references have addressed porphyrin molecules with multi "clips".[28−30] Here, we synthesized a derivative of porphyrin, tetra[*p*-(3-mercaptopropyloxy)phenyl]porphyrin (PPS_4), with four "clips", and examined its SAMs and properties. For comparison, 5-[*p*-(mercaptopropyloxy)phenyl]-10,15,20-triphenylporphyrin (PPS_1) with one "clip", was also synthesized and studied (Scheme 1). The results suggested PPS_4 could form more high density SAMs on gold surface than that of PPS_1, wherein the molecules oriented on substrates with a tilted angle. Moreover, SAMs of PPS_4 could generate nice nanojunctions based on gold nanogap electrodes (gap width: ca. 100 nm), which could be switched between low/high impedance states with light on/off as nanometer scaled photoswitchers.

* To whom correspondence should be addressed. Phone: +86-931-7971276. Fax: +86-931-7971323. E-mail: luxq@nwnu.edu.cn. Phone: +86-10-82615030. Fax: +86-10-62527925. E-mail: huwp@iccas.ac.cn.
† Northwest Normal University.
‡ Chinese Academy of Sciences.
§ National Center for Nanoscience and Technology.
⊥ NTT.

Experimental Section

Materials. PPS_1 and PPS_4 were synthesized as described elsewhere.[31,32] For the synthesis of PPS_1, first, predistilled pyrrole (9.0 mL, ca.0.133 mol) was added dropwise to 300.0 mL of refluxing propionic acid solution dissolving with 6.95 g (ca.0.0573 mol) of *p*-hydroxylbenzaldehyde and 6.0 g (ca.0.0573 mol) of benzaldehyde, and then refluxing for 1 h, evaporating the solvent in vacuo, separating by silica gel column chromatography with chloroform ($CHCl_3$) as the eluent, and further purifying by recrystallization from methanol. Second, the compound (100 mg, 0.15 mmol) was dissolved in DMF (30 mL) and K_2CO_3 (1 g) and 1,3-dibromopropylane (0.5 mL) were added. The reaction mixture was stirred at room temperature for 3 h. After extracting, evaporating, and purifying, K_2CO_3 (1 g) and thiol acetic (0.5 mL) in chloroform were added, refluxing 30 min, and then extracting, evaporating, and purifying again. Finally, the compound was dissolved in a mixed solvent of chloroform (50 mL) and methanol (15 mL), adding 1 g of KOH. After the hydrolysis reaction, the final product PPS_1 was obtained. IR spectroscopic (KBr pellet, cm^{-1}): $\upsilon_{(N-H)}$ pyrrole 3314; $\delta_{(N-H)}$ pyrrole 963 (in planarity); υ_{S-H} 2600; $\delta_{(C-O-C)}$ 1240; $\upsilon_{(C-H)}$ 2924; ^1H NMR ($CDCl_3$) δ 8.87 (d, 2H, J = 4.4 Hz, β-pyrrole-H), 8.85 (s, 4H, β-pyrrole-H), 8.84 (d, 2H, J = 4.4 Hz, β-pyrrole-H), 8.23 (d, 2H, J = 4.4 Hz, aromatic-H), 8.22 (d, 2H, J = 4.4 Hz, aromatic-H), 7.78−7.25 (m, 15H, aromatic-H), 4.40−1.54 (d, J = 14.2 Hz, 6H, $(CH_2)_3$−H), 0.86 (s, J = 14.2 Hz, 1H, S−H), −2.78 (s, 2H, N−H); UV/vis ($CHCl_3$) λ_{max} 418, 516, 552, 591, 648 nm.

PPS_4 was prepared and purified similarly to PPS_1 only without adding benzaldehyde in the first step (pyrrole:*p*-hydroxylbenzaldehyde = 1:1). IR spectroscopic (KBr pellet, cm^{-1}): $\upsilon_{(N-H)}$ pyrrole 3315; $\delta_{(N-H)}$ pyrrole 963 (in planarity); υ_{S-H} 2570; $\delta_{(C-O-C)}$ 1240; $\upsilon_{(C-H)}$ 2923; ^1H NMR ($CDCl_3$) δ 8.85 (d, 8H, J = 4.4 Hz, β-pyrrole-H), 8.11−7.98 (d, 8H, J = 4.4 Hz, aromatic-H), 7.29−7.08 (m, 8H, aromatic-H), 4.39−1.52 (d, J

10.1021/jp1020643
Published on Web 06/24/2010

SCHEME 1: Molecular Structures of PPS_1 and PPS_4

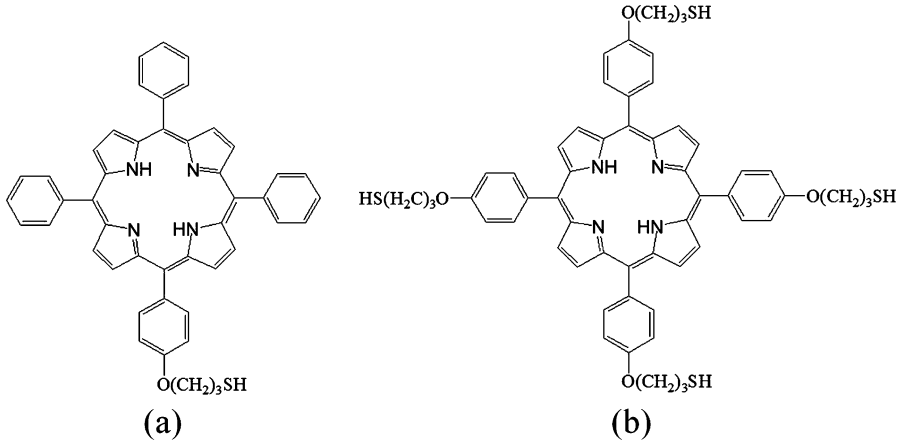

= 14.2 Hz, 24H, $(CH_2)_3$−H), 0.86−0.84 (s, J = 14.2 Hz, 4H, S−H), −2.78 (s, 2H, N−H); UV/vis ($CHCl_3$) λ_{max} 423, 519, 556, 593, 650 nm.

Sample Preparation. Gold films (15 nm) used for UV−vis measurements were prepared on Ti-primed (∼50 Å) quartz by thermal evaporation. Electrochemical cyclic voltammetry (CV) and *ac* impedance spectroscopy (EIS) were performed with a 3 mm diameter gold electrode,[33] which was immersed into a trichloromethane ($CHCl_3$) solution for 24 h self-assembly.

Characterization. Electrochemical experiments were carried out with a CHI 900. A gold (or SAMs on Au) electrode, a platinum wire, and a KCl saturated Ag/AgCl electrode were used as working, counter, and reference electrodes, respectively. Contact angle was perfomed with a Julabo F25, Germany. STM measurements were performed on Nanoscope IIIa Digital Instruments, using a typical constant current.

Au nanogap electrodes were prepared by electron beam lithography on Ti-primed (∼50 Å) oxidized silicon substrates (SiO_2: 300 nm), and the gap width was around 100 nm. The current−voltage (I−V) characteristics were recorded with a Keithley 4200 SCS and a Micromanipulator 6150 probe station in a clean and shielded box at room temperature in air.

Results and Discussion

Electrochemical Characterization. Figure 1a showed the CV curves obtained on bare Au and SAMs of PPS_1 and PPS_4 modified Au electrodes using $K_3Fe(CN)_6$ as the active molecules. For the bare Au electrode, there was a reversible electrochemical behavior, which was controlled by diffusion of a $[Fe(CN)_6]^{3-}/[Fe(CN)_6]^{4-}$ redox couple.[34,35] With PPS_1 and PPS_4 monolayers, the curves became flat, that is, the peak current decreased and the redox reaction became irreversible. This indicated the electron transport was blocked between $Fe(CN)_6^{3-}$ and the Au electrode.[36,37] Figure 1b shows the EIS plots of PPS_1 and PPS_4 monolayers and the bare Au electrode. For the bare Au electrode, a straight line at low frequency and a small semicircle at high frequency were observed in the Nyquist plots, demonstrating that process was assentially diffusion-controlled for the redox couple on the bare electrode. This was consistent with the results of CV on the bare Au electrode shown in Figure 1a. When SAMs of PPS_1 and PPS_4 respectively reached saturation after 24 h, a larger semicircle appeared at higher frequcency than that of the bare Au electrode, indicating the Au electrode was fully coated with SAMs. Comparing SAMs of PPS_1 with PPS_4, PPS_4 seemed more compact, because of its more flat (Figure 1a) curve and larger semicircle (Figure 1b). This was probably due to the stronger grafting ability of PPS_4 (four "clips" grafting) than that of PPS_1 (single "clip" grafting). Similarly, the SAMs of PPS_1 and PPS_4 were further characterized by Scanning Electrochemical Microscope (see the Supporting Information).

UV−Vis Characterization. UV−vis absorption spectra of PPS_1 and PPS_4 on the gold surface are shown in Figure 2. The inset image shows that the Soret band of SAMs of PPS_4 on the gold surface (solid line) was broadened and red-shifted by 13 nm relative to the corresponding spectra in $CHCl_3$ (dot line). Similar behavior was observed for SAMs of PPS_1 and in solution (not shown here), which demonstrated SAMs of PPS_4 formed

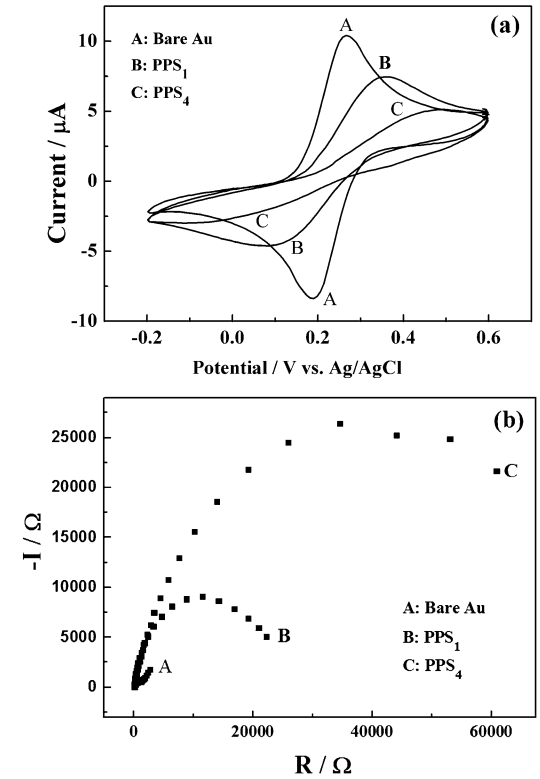

Figure 1. (a) Cyclic voltammetric current response versus applied bias for the bare electrode (A) and PPS_n (n = 1, 4) coated Au electrode (B and C). (b) Impedance plot of the bare electrode (A) and PPS_n (n = 1, 4) on the Au electrode (B and C); the electrode potential was 0.24 V (vs Ag/AgCl), the frequency range was 0.01 Hz to 10 Hz. The solution was 5 mM $Fe(CN)_6^{3-}$ with 0.05 M KCl as supporting electrolyte;, scan rate: 50 mV·S^{-1}.

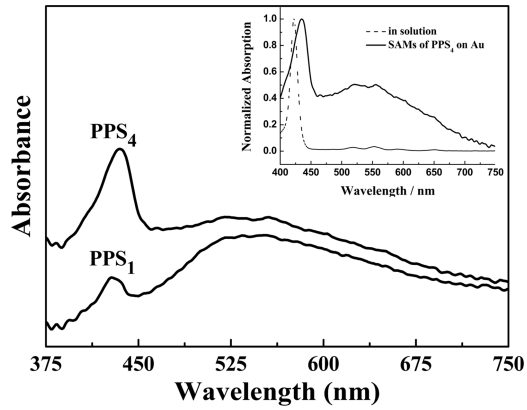

Figure 2. UV−vis spectra of SAMs of PPS_1 and PPS_4. Inset: UV−vis spectra of SAMs of PPS_4 and in $CHCl_3$.

SCHEME 2: SAM Model of PPS_4 on Au Surface

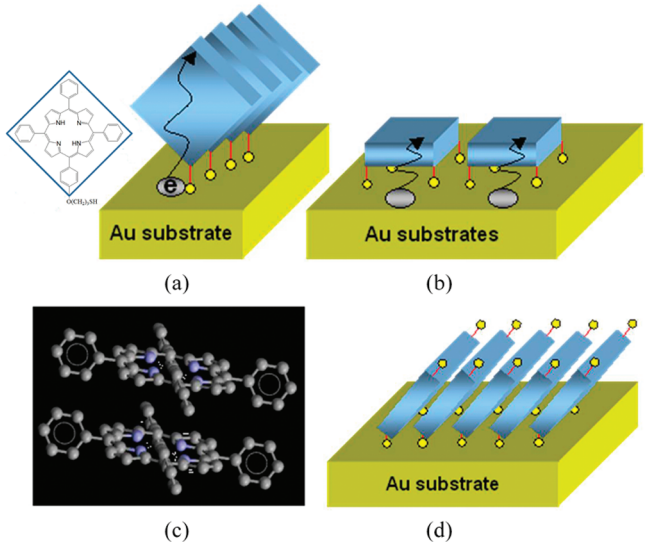

J-aggregate on the Au surface.[38] According to the absorbption of the Soret band at about 430 nm, the adsorption amount of porphyrin on the Au surface was calculated. The surface coverage of PPS_1 and PPS_4 was 1.45×10^{13} and 36×10^{13}molecules/cm^2, respectively; the results were consistent with ref 39, indicating the perpendicular arrangement of porphyrins on the Au surface. Compared to PPS_1, the surface coverage of PPS_4 was larger, i.e., more PPS_4 molecules absorbed on the Au surface, indicating the stronger grafting ability PPS_4 on Au than that of PPS_1 to form compact SAMs. The results accorded well with our electrochemical results.

Model of PPS_4 on the Au Surface. It was interesting to note the grafting states of PPS_1 and PPS_4 on the Au surface. As we know, the PPS_1 molecule stood on the Au surface in a tilted angle (Scheme. 2a) due to the grafting of its single "clip".[40,41] PPS_4 had four "clips", if every "clip" grafted on the Au surface, then the PPS_4 molecule would assemble on the Au surface as shown in Scheme 2b. As we know, electrons pass through SAMs by tunneling,[42,43] and the tunneling current is in inverse proportion with the thickness of SAM. Consider PPS_4 as a cube structure and the thickness of its SAMs in the b state in Scheme 2 is the height of PPS_4 (∼3.4 Å). But the thickness of PPS_1 SAMs is the length of the PPS_1 molecule with the side group length (∼3 nm). Therefore, the SAMs thickness of PPS_4 is much smaller than that of PPS_1, i.e., the tunneling current of PPS_4 SAMs (in Scheme 2, b state) should be much larger than that of PPS_1 (in Scheme 2, a state). But our actual electrochemical

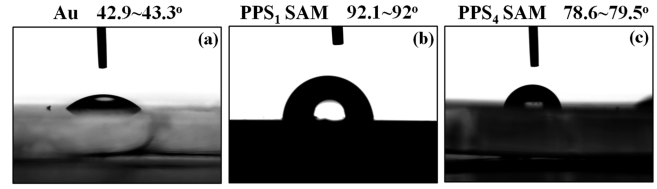

Figure 3. Contact angle of bare gold surface (a), Au-PPS_1 SAMs surface (b), and Au-PPS_4 SAMs surface (c).

results contradicted this analysis. Hence, the possibility of PPS_4 molecules grafted on the Au surface in the b state in Scheme 2 was very small. Instead, considering the inner porphyrin ring of PPS_4 has 22 π-electrons, the π-electrons of each PPS_4 will even reach 46 if we take account of the four peripheral phenyl groups of PPS_4. Therefore, the $\pi-\pi$ interaction between PPS_4 molecules should be very strong (Scheme 2c). Moreover, taking into account the space effect for molecular orientation in SAM, PPS_4 molecules were highly possibly arranged in the d state in Scheme 2, because the molecules $\pi-\pi$ interaction and orientation should be optimum although in this case two "clips" are probably hanging in the air.

Contact Angle and STM Study. To demonstrate this hypothesis, SAMs wettability and STM technique were applied for experiments. As we know, in PPS_4 end −SH groups are hydrophilic but the macro porphyrin ring should be hydrophobic. If PPS_4 molecules with −SH groups stretch out as in the Scheme 2d assumption, the SAMs should be more hydrophilic than PPS_1 SAMs. Figure 3 shows the contact angle of bare Au and Au-SAM surfaces of PPS_1 and PPS_4. The contact angle of SAMs of PPS_4 (78.6−79.5°) was smaller than that of SAMs of PPS_1 (92.1−92°), manifesting stronger hydrophilic SAMs of PPS_4 compared to SAMs of PPS_1. These results confirmed the above supposition in Scheme 2.

Figure 4a showed a typical constant current STM image of PPS_4 on Au (111), and Figure 4b was the sectional analysis of Figure 4a. It was obvious that close-packed monolayers of PPS_4 were formed on the gold surface with a few pinholes. The bright white dots in circles were probably physisorbed additional PPS_4 molecules on top of the existing PPS_4 monolayer. The large height step (white arrows) along the right side of the figure was due to the atomic step of the Au(111) substrate. The dark areas indicated by white rectangles are pinholes, corresponding to the uncovered gold surface. From the sectional analysis in Figure 4b, the apparent height of the PPS_4 in the SAM is measured to be 0.4 nm. Because of the coupling between the topographic contribution and the local electronic density of states, the exact physical height of the SAM is hard to obtain, while from the lower vertical distance, it could be hypothesized that the PPS_4 molecules in the SAM are tilted with a certain angle to the surface normal.[44−48] The two-alkane chains on the upper surface of the SAMs were probably entangled because of the weak van der Waals interactions of the short alkane chains and the large distance between alkyl chains. The well-packed monolayer was formed possibly with $\pi-\pi$ interaction between PPS_4 molecules, which agreed well with our above analysis.

Application of PPS_4 SAMs. For the potential application of assembled SAMs of PPS_4, a type of model device was described in Figure 5. The four thiol/thioacetyl-end-functionalized groups of PPS_4 were used as "clips" for adhesion to Au electrodes via Au−S bonds. To check the assembly effect of PPS_4 on Au electrodes, PPS_4 molecules were first cast on heated Au nanogap electrodes (inset of Figure 5) so that the PPS_4 solvent evaporated quickly, giving the PPS_4 molecules insufficient time for self-assembly. The current was rather small or even zero as shown

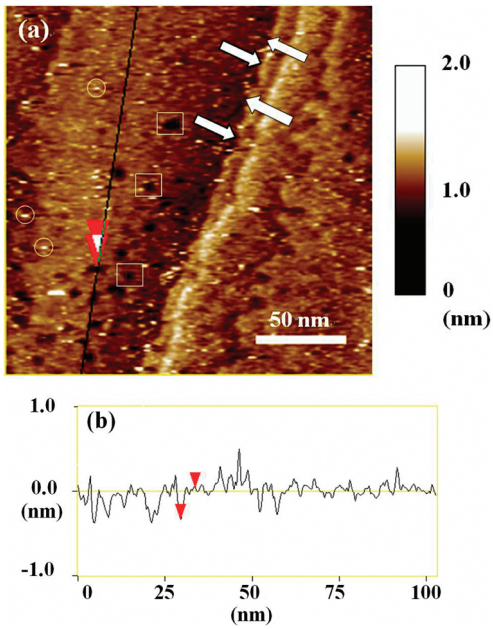

Figure 4. (a) Typical constant current image of PPS_4 on Au(111) observed. The image was obtained with a Pt/Ir tip at sample bias voltage of 811.8 mV and tunneling current of 341.8 pA. The *Z* data scale is 2.00 nm, and the scan size is 144.1 nm × 144.1 nm. The linear features indicated by white arrows are attributed to the atomic step of the Au(111) substrate. The dark areas indicated by small white rectangles are pinholes on the substrate. And bright white dots in circles are physisorbed PPS_4 molecules, which are remnant ones even after ultrasonication treatment (about 2 min). (b) Sectional analyses for panel a. The tags indicate the positions for measuring vertical distance along the selected line.

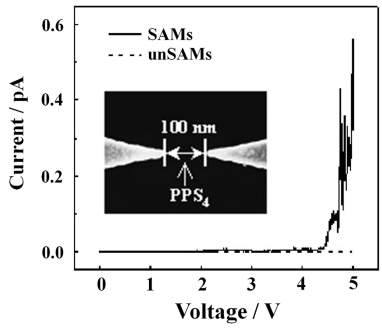

Figure 5. *I*−*V* characteristics of a PPS_4 connected nanojunction under ambient conditions.

in Figure 5. But after treating the Au/PPS_4/Au nanojunctions in $CHCl_3$ vapor (in a bottle $^1/_3$ filled with $CHCl_3$) for a further 24 h and keeping them in a vacuum chamber for 24 h, (i) the current of the treated sample was much larger than that of the untreated devices and (ii) nonlinear stepwise characteristics appeared in the treated devices with the applied bias as shown in Figure 5. The nonlinear stepwise characteristics of our devices were probably due to tunneling injection through the Au/PPS_4 interface. There are a number of reports on electrons tunneling phenomena in thiol-based organic nano/molecular junctions.[49−58] It is reported that the geometry of the orbitals on the sulfurs does not permit the conjugated π-orbitals from the PPS_4 molecules to interact strongly with the conduction orbitals of the gold electrodes. The orbital mismatch creates a potential barrier at the interface of the Au-PPS_4. A self-assembled nanojunction is similar to a quantum dot junction. In the junction, the self-assembly PPS_4 molecules acted as a quantum dot and the terminal sulfur atoms acted as two tunnel barriers.

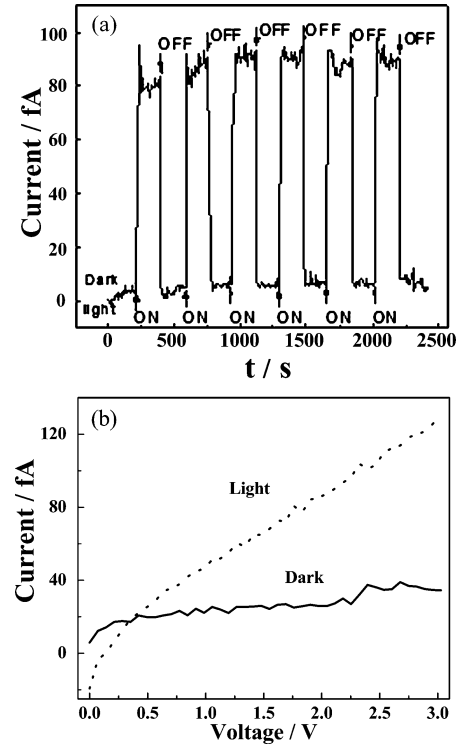

Figure 6. (a) Photoresponse characteristics (white light, 57.6 mW) of the nanojunction and (b) *I*−*V* characteristics of the nanojunction with and without photoirradiation.

Therefore, electrons of the treated devices observing nonlinear stepwise characteristics were transported by tunneling injection through the Au−S bond, and the current was much low below 4 V due to the energy barrier between Au electrodes and PPS_4 molecules.

The photoresponse behavior of the self-assembled Au/PPS_4/Au nanojunction under light irradiation was shown in Figure 6a. With the light on/off, the nanojunction was capable of switching between low/high impedance states as a nanometer-scale photoswitch (the voltage between the two electrodes was kept constant at 3 V). The nanojunction displayed two "distinct" states: (i) a "low"-current state under dark conditions and (ii) a "high"-current state under light conditions. The switching in those two states was both reversible and fast. In the "off" state, the resistance was as high as $\sim 6 \times 10^{14}$ Ω. In the "on" state, the resistance was only $\sim 3 \times 10^{13}$ Ω, and the switching ratio is 20. This photoswitching occurred because PPS_4 was a good photoconductor. Under illumination, photon-generated excitons will dissociate into free electrons and free holes resulting in increased current. The photo and dark currents of the self-assembled nanojunction are shown in Figure 6b.

Conclusions

Good SAMs of PPS_4 on gold surfaces were identified by UV−vis, CVs, EIS, contact angle, and STM. PPS_4 molecules were oriented in SAMs with a titled angle. Self-assembled nanojunctions of PPS_4 were fabricated by using gold nanogap electrodes. The nanojunctions exhibited nonlinear current−voltage characteristics, indicating the possibility of current injection from Au electrodes into PPS_4 by tunneling. With the light on/off, the nanojunctions switched between low/high impedance states and operat as nanometer scaled photoswitchers.

Acknowledgment. The authors acknowledge financial support from the Natural Science Foundation of China (20775060,

20875077, 209270004, 20965007, and 20945003), the Natural Science Foundation of Gansu Province (0701RJZA109, 0803RJZA105, 096RJZA121, and 096RJZA122), the key progress of the Education Committee (08_{ZX}-07) of Gansu, and the key Laboratory of Polymer Materials of Gansu Province, China.

Supporting Information Available: Characterization SAMs of PPS_4 by scanning electrochemical microscope. This material is available free of charge via the Internet at http://pubs.acs.org.

References and Notes

(1) Drain, C. M. *Proc. Natl. Acad. Sci. U.S.A.* **2002**, *99*, 5178–5182.
(2) Kurreck, H.; Huber, M. *Angew. Chem., Int. Ed.* **1995**, *34*, 849–866.
(3) Kuramochi, Y.; Satake, A.; Kobuke, Y. *J. Am. Chem. Soc.* **2004**, *126*, 8668–8669.
(4) Ulman, A. *Chem. Rev.* **1996**, *96*, 1533–1554.
(5) Tour, J. M. *Chem. Rev.* **1996**, *96*, 537–554.
(6) Whitesides, G. M.; Mathias, J. P.; Seto, C. T. *Science.* **1991**, *254*, 1312–1319.
(7) Zareie, M. H.; Ma, H.; Reed, B. W.; Jen, A. K. Y.; Sarikaya, M. *Nano Lett.* **2003**, *3*, 139–142.
(8) Falk, J. E. *Porphyrins and Metalloporphyrins*; Elsevier: Amsterdam, The Netherlands, 1964.
(9) Smith, K. M. *Porphyrins and Metalloporphyrins*; Elsevier: Amsterdam, The Netherlands, 1975.
(10) Dolphin, D. *The Porphyrins*; Academic: New York, 1978.
(11) Kampas, F. J.; Yamashita, K.; Fajer, J. *Nature* **1980**, *284*, 40–42.
(12) Schlettwein, D.; Kaneko, M.; Yamada, A.; Wohrle, D.; Jaeger, N. I. *J. Phys. Chem.* **1991**, *95*, 1748–1755.
(13) McDermott, M. T.; Green, J. B. D.; Porter, M. D. *Langmuir* **1997**, *13*, 2504–2510.
(14) Zhang, Z.; Hu, R.; Liu, Z. *Langmuir* **2000**, *16*, 1158–1162.
(15) Kamil, Z.; Pavel, M.; Radko, V.; Karel, V.; Vladimlr, K.; Jonathan, L. S. *Langmuir* **2002**, *18*, 6896–6906.
(16) Antonino, G.; Sebastiano, B.; Placido, M.; Emilio, S.; Daniele, V.; Ignazio, F. *Chem. Mater.* **2005**, *17*, 521–526.
(17) Shimazu, K.; Takechi, M.; Fujii, H.; Suzuki, M.; Saiki, H.; Yoshimura, T.; Uosaki, K. *Thin Solid Films* **1996**, *273*, 250–253.
(18) Boeckl, M. S.; Bramblett, A. L.; Hauch, K. D.; Sasaki, T.; Ratner, B. D.; Rogers, J. W. *Langmuir* **2000**, *16*, 5644–5653.
(19) Ishida, A.; Sakata, Y.; Majima, T. *Chem. Commun.* **1998**, 57–58.
(20) Cordas, C. M.; Viana, A. S.; Leupold, S.; Montforts, F. P.; Abrantes, L. M. *Electrochem. Commun.* **2003**, *5*, 36–41.
(21) Hutchison, J. E.; Postlethwaite, T. A.; Murray, R. W. *Langmuir* **1993**, *9*, 3277–3283.
(22) Zak, J.; Yuan, H.; Ho, M.; Woo, L. K.; Porter, M. D. *Langmuir* **1993**, *9*, 2772–2774.
(23) Van Galen, D. A.; Majda, M. *Anal. Chem.* **1988**, *60*, 1549–1553.
(24) Katz, E.; Willner, I. *Langmuir* **1997**, *13*, 3364–3373.
(25) Uosaki, K.; Kondo, T.; Zhang, X. Q.; Yanagida, M. *J. Am. Chem. Soc.* **1997**, *119*, 8367–8368.
(26) Imahori, H.; Norieda, H.; Ozawa, S.; Ushida, K.; Yamada, H.; Azuma, T.; Tamaki, K.; Sakata, Y. *Langmuir* **1998**, *14*, 5335–5338.
(27) Imahori, H.; Hosomizu, K.; Mori, Y.; Sato, T.; Ahn, T.; Kim, S. K.; Kim, D.; Nishimura, Y.; Yamazaki, I.; Ishii, H.; Hotta, H.; Motano, Y. *J. Phys. Chem. B* **2004**, *108*, 5018–5025.
(28) Postlethwaite, T. A.; Hutchison, J. E.; Hathcock, K. W.; Murray, R. W. *Langmuir* **1995**, *11*, 4109–4116.
(29) Tomizaki, K.; Yu, L. H.; Wei, L. Y.; Bocian, D. F.; Lindsey, J. S. *J. Org. Chem.* **2003**, *68*, 8199–8207.
(30) Amir, A.; Yasseri, D. S.; Malinovskii, V. L.; Loewe, R. S.; Lindsey, J. S.; Zaera, F.; Bocian, D. F. *J. Am. Chem. Soc.* **2004**, *126*, 11944–11953.
(31) Lu, X. Q.; Geng, Z. X.; Wang, Y. S.; Lv, B. Q.; Kang, J. W. *Synth. React. Inorg. M.* **2002**, *32*, 843–851.
(32) Zuo, G. F.; Lu, X. Q.; Xue, Z. H.; Lv, B. Q.; Wang, Y. S.; Kang, J. W. *Synth. React. Inorg., Met.-Org., Nano-Met. Chem.* **2006**, *36*, 589–594.
(33) Wang, Y. L.; Gan, L. F.; Chen, H. J.; Dong, S. J.; Wang, J. *J. Phys. Chem. B* **2006**, *110*, 20418–20425.
(34) Valber, A. P.; Thiago, R. L. C.; Paixao, R. S.; Freire, M. B. *J. Electroanal. Chem.* **2007**, *602*, 149–155.
(35) Randriamahazaka, H. N. *J. Electroanal. Chem.* **2009**, *632*, 1–7.
(36) Bollo, S.; Yãñez, C.; Sturm, J.; Núñez-Vergara, L.; Squella, J. *Langmuir* **2003**, *19*, 3365–3370.
(37) Nahir, T. M. *Langmuir* **2002**, *18*, 5283–5286.
(38) Khairutdinov, R. F.; Serpone, N. J. *J. Phys. Chem. B* **1999**, *103*, 761.
(39) Bramblett, A. L.; Boeckl, M. S.; Hauch, K. D.; Ratner, B. D., Jr. *Surf. Interface Anal.* **2002**, *33*, 506–515.
(40) Hutchison, J. E.; Postlehwaite, T. A.; Chen, C. H.; Hathcock, K. W.; Ingram, R. S.; Ou, W.; Linton, R. W.; Murray, R. W. *Langmuir* **1997**, *13*, 2143–2148.
(41) Guo, L. H.; Mclendon, G.; Razafitrimo, H.; Gao, Y. L. *J. Mater. Chem.* **1996**, *6*, 369–374.
(42) Reed, M. A.; Zhou, C.; Muller, C. J.; Burgin, T. P.; Tour, J. M. *Science* **1997**, *278*, 252–254.
(43) Lu, X. Q.; Li, M. R.; Yang, C. H.; Zhang, L. M.; Li, Y. F.; Jiang, L.; Li, H. X.; Jiang, L.; Liu, C. M.; Hu, W. P. *Langmuir* **2005**, *22*, 3035–3039.
(44) Duong, B.; Arechabaleta, R.; Tao, N. J. *J. Electroanal. Chem.* **1998**, *447*, 63–69.
(45) Scudiero, L.; Barlow, D. E.; Mazur, U.; Hipps, K. W. *J. Am. Chem. Soc.* **2001**, *123*, 4073–4080.
(46) Walzer, K.; Marx, E.; Greenham, N C.; Less, R. J.; Raithby, P. R.; Stokbro, K. *J. Am. Chem. Soc.* **2004**, *126*, 1229–1234.
(47) Bumm, L. A.; Arnold, J. J.; Dunbar, T. D.; Allara, D. L.; Weiss, P. S. *J. Phys. Chem. B* **1999**, *103*, 8122–8127.
(48) Barlow, D. W.; Scudiero, L.; Hipps, K. W. *Langmuir* **2004**, *20*, 4413–4421.
(49) Andres, R. P.; Bein, T.; Dorogi, M.; Feng, S.; Henderson, J. I.; Kubiak, C. P.; Mahoney, W.; Osifchin, R. G.; Reifenberger, R. *Science* **1996**, *272*, 1323–1325.
(50) Yaliraki, S. N.; Kemp, M.; Ratner, M. A. *J. Am. Chem. Soc.* **1999**, *121*, 3428–3434.
(51) Nitzan, A. *Annu. Rev. Phys. Chem.* **2001**, *52*, 681–750.
(52) Petrov, E. G.; Haenggi, P. *Phys. Rev. Lett.* **2001**, *86*, 2862–2865.
(53) Kushemerick, J. G.; Holt, D. B.; Yang, J. C.; Naciri, J.; Moore, M. H.; Shashidhar, R. *Phys. Rev. Lett.* **2002**, *89*, 086802−086805.
(54) Xu, B. Q.; Tao, N. J. *Science* **2003**, *301*, 1221–1223.
(55) Hu, W. P.; Nakashima, H.; Furukawa, K.; Kashimura, Y.; Ajito, K.; Torimitsu, K. *Appl. Phys. Lett.* **2004**, *85*, 115–117.
(56) Hu, W. P.; Nakashima, H.; Furukawa, K.; Kashimura, Y.; Ajito, K.; Liu, Y. Q.; Zhu, D. B.; Torimitsu, K. *J. Am. Chem. Soc.* **2005**, *127*, 2804–2805.
(57) Hu, W. P.; Jiang, J.; Nakashima, H.; Luo, Y.; Kashimura, Y.; Chen, K. Q.; Shuai, Z.; Lu, W.; Liu, Y. Q.; Zhu, D. B.; Torimitsu, K. *Phys. Rev. Lett.* **2006**, *96*, 027801−027804.
(58) Chen, J.; Reed, M. A.; Rawlett, A. M.; Tour, J. M. *Science* **1999**, *286*, 1550–1552.

JP1020643